

## Microstructure and properties of an Al-7.5Zn-1.7Mg-1.4Cu-0.12Zr alloy

Xiwu Li, Baiqing Xiong, Yongan Zhang, Zhihui Li, Baohong Zhu, Feng Wang, Hongwei Liu  
State Key Laboratory for Fabrication and Processing of Nonferrous Metals,  
General Research Institute for Nonferrous Metals, Beijing, China

The microstructure and properties of an Al-7.5Zn-1.7Mg-1.4Cu-0.12Zr alloy in T6 and T7X tempers have been investigated using TEM, mechanical properties testing, conductivity measurement, fracture toughness testing, fatigue testing, slow strain rate testing and soaking quench method etc. The results indicate that T6 temper can greatly increase the strength of the alloy, but with the lowest SCC resistance. When T7X tempers are performed, the alloy can obtain a good comprehensive performance with GPII zones,  $\eta'$  phases and  $\eta$  phases as the major precipitates in the matrix and coarser and discontinuous precipitates on the grain boundaries. It is shown that the T7X tempers can improve SCC resistance of the alloy. The alloy also exhibits a good combination of fracture toughness and fatigue resistance. The alloy in T74 temper presents high fatigue strength of  $10^7$  cycles, which are 290 MPa for a notch factor  $K_t=1$  and 95 MPa for a notch factor  $K_t=3$ , respectively. And the alloy has a good quench performance, after soaking quenched in water, the strength of the forging with 210mm thickness is stable and varies less than 10% along the depth direction.

**Keywords:** Al-Zn-Mg-Cu alloy, Microstructure, Properties, Aging treatment.

### 1. Introduction

Al-Zn-Mg-(Cu) (7xxx series) alloys are typical aging precipitation strengthening alloys, with a vast number of applications in the aerospace industry. Recently, in the aerospace industry there is a trend to the substitution of assemblies and built-up structures by so-called integral or monolithic structures with the advantage of weight reduction and production cost savings due to the lower number of joints and components, which requires very heavy aluminum forgings and plates with larger cross sections (150~300 mm) and increased property requirements [1-4]. To meet the stringent property requirements at the center of the thick sections, General Research Institute for Non-ferrous Metals has started developing an Al-7.5Zn-1.7Mg-1.4Cu-0.12Zr alloy with even lower quench sensitivity and a much higher strength-toughness combination through modifications in solute content and in particular in Zn/Mg/Cu ratios by phase diagram work. The alloy was developed by studying various chemical compositions, fabrication and heat treatments [5-7]. In this study, the microstructure, tensile strength, corrosion properties of the alloy in different tempers have been investigated, and toughness, fatigue and quench performance of the alloy have been evaluated as well.

### 2. Experimental procedures

The composition of the alloy was 7.5wt% Zn, 1.7wt% Mg, 1.4wt% Cu, 0.12wt% Zr, 0.02wt% Fe, 0.01wt% Si and balance Al. Ingots of approximately  $\phi 210$  mm were produced by semi-continuous casting. After casting, the alloy were homogenized at 440°C for 12 h plus 475°C for 24 h and then hot extruded into 102 mm  $\times$  25 mm thick plate. Specimens were solution heat treated at 475°C for 50~120 min and then water quenched to RT. For the one-step aging, the samples were aged at 120°C for 24 h (T6 temper). For the two-step aging, the samples were aged at 110°C for 6 h and then aged at 160°C for 6h (T76 temper), 10h (T74 temper) and 16h (T73 temper), respectively.

The mechanical properties (according to GB/T 228), electrical conductivity (MS/m, according to GB/T 12966), Fracture toughness ( $K_{IC}$ , according to GB/T 4161) and fatigue properties (according to

GB/T 3075) were determined for selected conditions. A JEM-2000FX transmission electron microscope (TEM) and a JEM-2010 high-resolution electron microscope (HREM) were used for observing microstructure. In order to compare fracture toughness of the alloy with other 7xxx Al series alloys, an aluminum 7150 alloy (AA7150, Al-6.4Zn-2.3Mg-2.3Cu-0.12Zr) with the same processes was applied.

The SCC susceptibility was studied by slow strain rate testing (SSRT) in a 3.5% NaCl solution adjusted to a pH of 3.0 by the addition of HCl solution. Identical tests were carried-out in dry air. The tests were carried-out under displacement control on a WDML-3 machine at an initial strain rate of  $0.5 \times 10^{-6} \text{ s}^{-1}$ . The SCC susceptibility can be assessed by an equation of the form,

$$I_{SSRT} = 1 - [\sigma_{fw} \cdot (1 + \delta_{fw})] / [\sigma_{fA} \cdot (1 + \delta_{fA})] \quad (1)$$

Where  $I_{SSRT}$  is known as the stress corrosion factor;  $\sigma_{fw}$  is the fracture strength of the specimen in corrosion solution (MPa);  $\sigma_{fA}$  is the fracture strength of the specimen in dry air (MPa);  $\delta_{fw}$  is the elongation of the specimen in corrosion solution (%);  $\delta_{fA}$  is the elongation of the specimen in dry air (%). At least three specimens of a given heat-treatment were tested under each environmental condition.

In the present study, the quench sensitivity of the alloy was investigated by the soaking quench method. An as-special treated sample block with dimensions 200 (L)  $\times$  200 (LT)  $\times$  210 (ST) mm<sup>3</sup> cut from a forging with 210 mm thickness was subjected to soaking quench test following the solution heat treatment to simulate the quenching of a whole forging with a thickness of 210 mm. The tensile properties and electrical conductivity were measured after T6 temper treatment at different distances from the quenched surface were used to assess the quench sensitivity of the alloy.

### 3. Results and Discussion

#### 3.1 Microstructure

Fig. 1 shows the morphology and distribution of precipitates in the alloy in several representative tempers. It was found that the precipitates in both the matrix and the grain boundary become coarser with increasing over-aging degree from T6 temper to T74 temper and then to T73 temper, while the precipitation free zone (PFZ) is present. After aging for 24 h at 120°C, dark round precipitates with a diameter of 2~7 nm are observed in BF images. The grain boundary precipitates are continuous and narrow without the PFZ, as shown in Fig. 1(a). When T74 temper is performed on the alloy, the precipitates grow obviously, their size is about 4~15 nm, as shown in Fig. 1(b). After T73 temper treatment, the precipitates grow up to 5~20 nm with a little lower number density, and the grain boundary precipitates become coarser, discontinuous and the width of the PFZ increases obviously, which is up to 40~50 nm approximately, as shown in Fig. 1(c). In general, the microstructure of the grain boundaries plays an important role in the development of stress corrosion cracking (SCC). In T6 temper, the continuous grain boundary precipitates accelerated the rate of crack propagation, which led to a degradation of the SCC resistance. In T7X tempers, the discontinuous and growing grain boundary precipitates have been suggested to reduce the susceptibility to SCC.

Fig. 2 shows further that the image and SAED patterns of precipitates in the alloy in T74 temper. From the SAED patterns, as shown in Fig.2(b,c), the diffraction features of the  $\eta'$  phases were clearly observed, such as some diffraction spots and stronger streaks along  $\{111\}$  direction at 1/3 and 2/3 of the  $\{220\}$  positions in  $[001]_{Al}$  and  $[112]_{Al}$  direction. Some of the spots were caused by the diffraction of  $\eta$  phases. And diffraction spots near 1/2  $\{311\}$  in  $[112]_{Al}$  direction associated with the GPII zones were clearly observed. It also can be noted that the presence of sharp diffraction spots at  $\{110\}$  positions in  $[112]_{Al}$  direction, which are associated with spherical  $Al_3Zr$  dispersoids [8-10]. The results of the SAED analysis can be confirmed by HREM work, as shown in Fig. 3. Contrast features in the  $[110]$  projection, Fig.3 (a), were identified as GPII zones, which appear as thin objects parallel

to  $\{111\}$  planes, about 2-4 atom layers thick. And some larger particles approximately 7-16 atom layers thick were found, Fig.3 (b), the semi-coherent  $\eta'$  phase can be identified. As shown in Fig. 3(c), round-like particle can be observed, indicating non-coherency with the matrix, which can be identified as  $\eta$  phase [8-11]. It indicated that in the T74 temper the main precipitates are GPII zones,  $\eta'$ , and  $\eta$  phases.

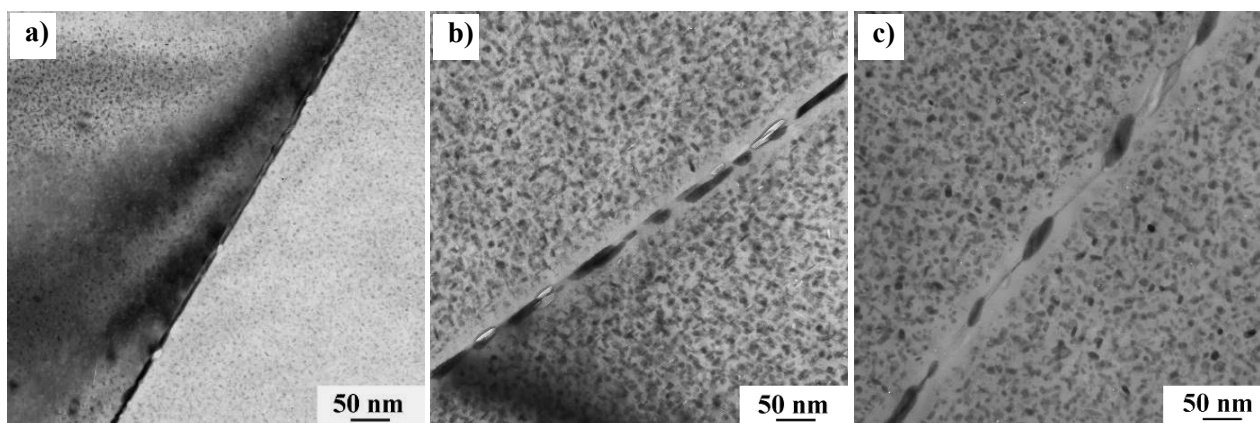


Fig.1 TEM BF images of the alloy in different tempers  
a) T6 (120°C/24h); b) T74 (110°C/6h+160°C/10h); c) T73 (110°C/6h+160°C/16h)

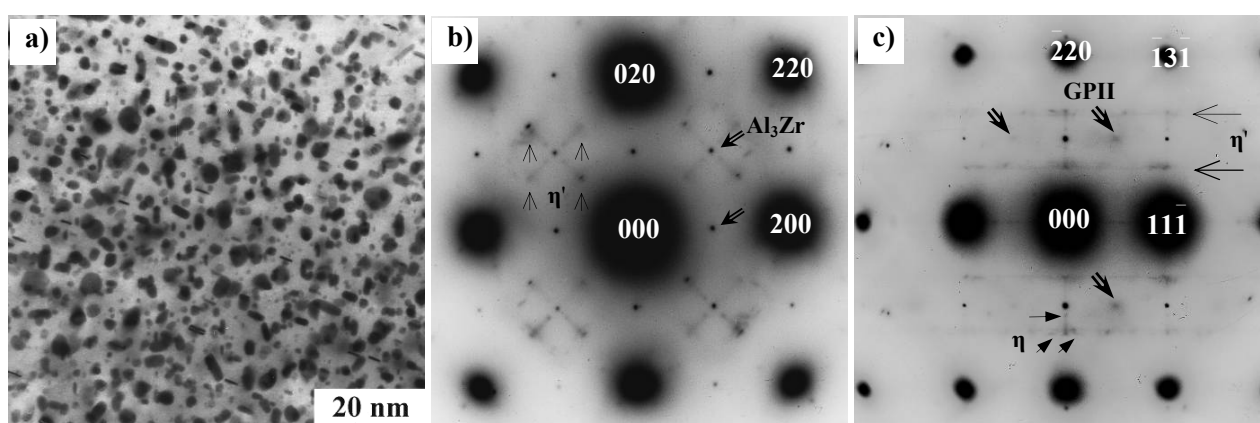


Fig.2 TEM BF image and SAED patterns of the alloy in T74 temper  
a) BF image; b) SAED pattern in  $[001]_{Al}$ ; c) SAED pattern in  $[112]_{Al}$

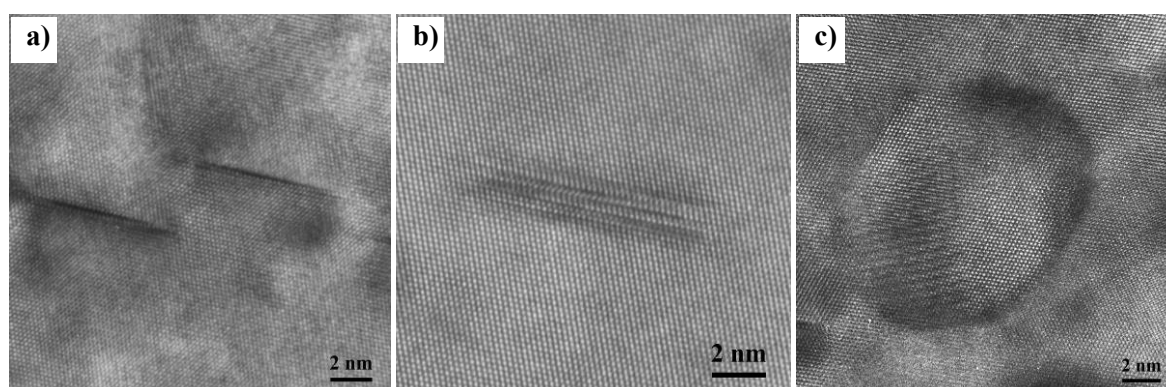


Fig.3 HREM images in  $[110]_{Al}$  of precipitates of the alloy in T74 temper  
(a) Image of the GPII zones; (b) Image of the  $\eta'$  phase; (c) Image of the  $\eta$  phase

### 3.2 Properties

The tensile properties and electrical conductivity of the alloy in different tempers are given in Table 1. It is found that a relatively high strength level of the alloy can be achieved in T6 temper, but with low conductivity level. When T7X tempers are performed, electrical conductivity of the alloy increase obviously, which is up to 25.0 MS/m, but in this case, 8%~16% loss in tensile strength was inevitable. It is known that electrical conductivity serves as an indicator of SCC resistance [12]. The SCC resistance has been found to increase with the increasing of electrical conductivity in Al-Zn-Mg-Cu alloys. In the present study, the electrical conductivity of the alloy in T7X tempers has considerably increased compared to that in T6 temper, suggesting that the alloy in T7X tempers can get an improved SCC resistance. This prediction can be confirmed by slow strain rate testing (SSRT). The results of the SSRT are listed in Table 2. It can be found that the alloy in T6 temper show more susceptibility to SCC than the alloy in T7X tempers.

Table 1 Mechanical properties and electrical conductivity of the alloy in various tempers

Aging temper	UTS (MPa)	TYS (MPa)	Elongation (%)	Electrical conductivity (MS/m)
T6 (120°C/24h)	590	540	16.5	20.3
T76 (110°C/6h+160°C/6h)	550	520	17.3	23.4
T74 (110°C/6h+160°C/10h)	520	485	18.0	24.3
T73 (110°C/6h+160°C/16h)	500	460	17.0	25.0

Table 2 Stress corrosion factor ( $I_{SSRT}$ ) in 3.5% NaCl solution of the alloy in different tempers

Temper	T6	T76	T74	T73
$I_{SSRT}$	0.172	0.090	0.063	0.036

The fracture toughness properties of the alloy and AA 7150 are presented in Table 3. AA7150 in this study can obtain good fracture toughness, higher than that as mentioned in reference. There were only reference values for the alloy because of  $P_{max}/P_q \leq 1.1$  resulting from the appearance of necking down during fracture toughness test. But in the same treatment and measurement condition it can be qualitatively reveal that the alloy has quite excellent fracture toughness, whose  $K_{IC}$  values are higher than that of AA 7150 obtained from the same processing.

Table 3 Fracture toughness properties (L-T position) of the alloy and AA 7150 obtained from the same processing

Alloy	Temper	$K_{IC}$ [Mpa.m <sup>1/2</sup> ]		Remark
		Experiment data	Literature [8]	
AA 7150	T6 (120°C/24h)	44	22~24 (T77)	True value
The alloy	T6 (120°C/24h)	70	-	Reference value

The S-N curves for fatigue properties of the alloy in T74 temper is plotted in Fig.4. Specimens from the L-direction were tested with notch factor  $K_t=1$  and  $K_t=3$  and an R-value of 0.1. For the alloy a high fatigue life is observed. The fatigue strength of  $10^7$  cycles is nearly 290 MPa for a notch factor  $K_t=1$  and 95 MPa for a notch factor  $K_t=3$ , respectively.

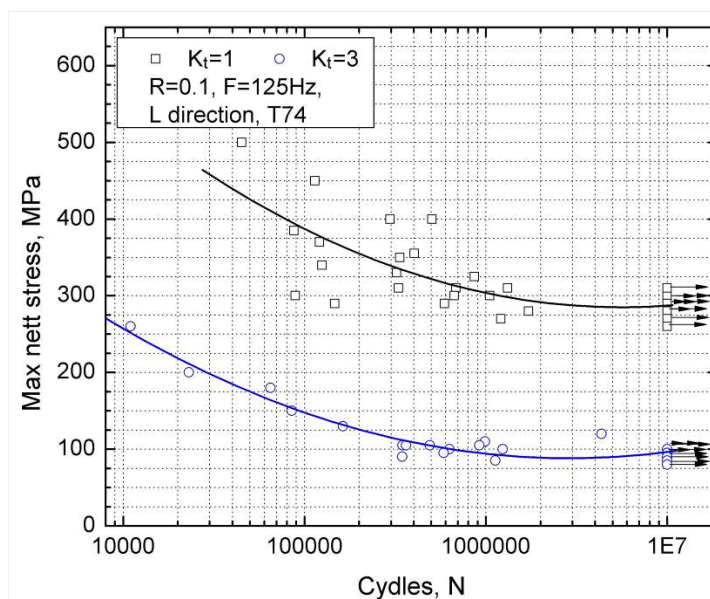


Fig.4 S-N curves of the novel alloy in T74 temper at the different  $K_t$  levels

Fig.5 shows properties profiles for the soaking quenched block mimicking a forging with a thickness of 210 mm along the depth direction. It can be found that after soaking quenched in water, the strength of the forging with 210mm thickness in T74 temper is stable and varies less than 10% along the depth direction; if the strength of the secondary external layer (distance from quenched surface is approximate to 20 mm) of the forging is defined as evaluation criterion, the strength of the forging varies less than 5%, which reveal that the alloy has a good quench performance.

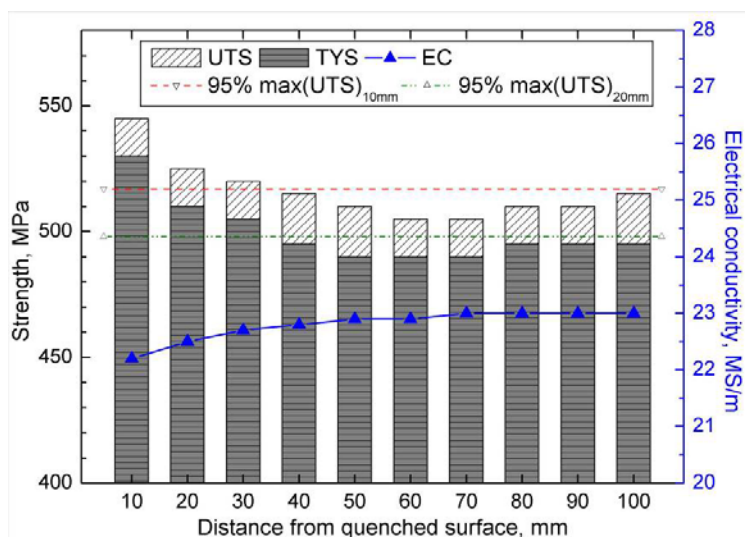


Fig.5 Properties profiles of the test specimens of the alloy along the depth direction

#### 4. Summary

After T6 temper treatment, the alloy can get a very fine distribution of precipitates inside grains, with a relatively high strength level, but with the lowest SCC resistance. When T7X tempers are performed, the alloy can obtain a good comprehensive performance with GPII zones,  $\eta'$  phases and  $\eta$  phases as the major precipitates in the matrix and coarser and discontinuous precipitates on the grain boundaries. The UTS, TYS, elongation and electrical conductivity values of the alloy in T74 were 520 MPa, 485 MPa, 18.0% and 24.3 MS/m, respectively. It is shown that the T7X tempers can

improve SCC resistance of the alloy. The alloy also exhibits a good combination of fracture toughness and fatigue resistance. The alloy in T74 temper presents high fatigue strength of  $10^7$  cycles, which are 290 MPa for a notch factor  $K_t=1$  and 95 MPa for a notch factor  $K_t=3$ , respectively. The alloy has a good quench performance, after soaking quenched in water, the strength of the forging with 210mm thickness is stable and varies less than 10% along the depth direction.

### Acknowledgement

This work was supported by the National High-Tech Research Development Program of China (Grants No. 2008AA03Z506) and National Natural Science Foundation of China (Grants No. 50904010). The authors are also grateful to professors Ansheng Liu, Zhiwei Du and Beiling Shao for the TEM work.

### References

- [1] L. John: Mater. Sci. Forum. 519-521 (2006) 1233-1238.
- [2] T. Warner: Mater. Sci. Forum, 519-521 (2006) 1271-1278
- [3] D.J. Chakrabarti, J. Liu, R.R. Sawtell, et al.: Aluminium Alloys, Ed. by J. F. Nie, A. J. Morton and B. C. Muddle (Institute of Materials Engineering Australasia Ltd, 2004) pp. 969-974.
- [4] M. Hilpert, G. Terlinde, T. Witulski, et al.: *Aluminium Alloys*, Ed. by J. Hirsch, B. Skrotzki and G. Gottstein, (WILEY-VCH, Weinheim, 2008) pp. 209-214.
- [5] X. W. Li, B. Q. Xiong, Y. A. Zhang, et al.: Sci. in China Ser. E-Tech. Sci. 52 (2009) 67-71.
- [6] X. W. Li, B. Q. Xiong, Y. A. Zhang, et al.: Int. J Mod. Phys. B. 23 (2009) 900-905.
- [7] B. Q. Xiong, X. W. Li, Y. A. Zhang, et al.: Chinese J Nonferrous Metals. 19 (2009) 1539-1547.
- [8] X. J. Jiang, B. Noble, B. Holme, et al.: Metall. Mater. Trans. A. 31 (2000) 339-348.
- [9] X. Z. Li, V. Hansen, J. Gjønnes, et. al.: Acta Mater. 47 (1999) 2651-2659.
- [10] S. Gang, C. Alfred: Acta Mater. 52 (2004) 4503-4516.
- [11] L.K. Berg, J. Gjønnes, V. Hansen, et al.: Acta Mater. 49 (2001) 3443-3451.
- [12] M. J. Starink, X. M. Li: Metall. Mater. Trans. A. 34 (2003) 899-905.